

Supplementary Material for:
Programmable photonic quantum walks on lattices with cyclic, toroidal, and cylindrical topology .

S1. PROPAGATION OF SCALAR WAVEPACKETS WITH ZERO GROUP VELOCITY IN CYCLIC LATTICES: PARABOLIC ENERGY BAND APPROXIMATION

As shown in the Methods, the probability of finding a particle in the lattice site m at the time step t is

$$P(m, t) = |\langle m | \psi_t \rangle|^2 = \left| \sum_h e^{iq_h m} e^{-(q_h - q_0)^2 \frac{w^2}{4}} e^{iE(q_h)t} \right|^2. \quad (\text{S1})$$

It is worth considering a further approximation, which consists in evaluating $P(m, t)$ using the expansion $E(q_h) = E(q_0) + 1/2(d^2E/dq^2)|_{q_0}(q_h - q_0)^2 \equiv E_0 + \beta(q_h - q_0)^2$, where the first-order term was neglected assuming zero group velocity. It follows that

$$P(m, t) \approx P_a(m, t) = \left| \sum_h e^{iq_h m} e^{-(q_h - q_0)^2 \left[\frac{w^2}{4} + i\beta t \right]} \right|^2. \quad (\text{S2})$$

This expression describes the wavepacket in terms of the group velocity dispersion β , the wavepacket's width w , and the sampling of the Brillouin zone q_h . We consider the cases $q_h(s) - q_0 = 2\pi h/N - s\pi/N$ with $s = 0, 1$ (corresponding, respectively, to $q_0 = \pi$ and $q_0 = 0$ in our experiment). Figure S1 shows the trend of $P(m, t)$ compared with the second-order approximation $P_a(m, t)$ for our protocol. We can see that $P_a(m, t)$ captures the main qualitative effects, i.e., that for $s = 1$ the wavepacket periodically tunnels between opposite positions in the lattice space, while for $s = 0$ it periodically splits in two lobes then refocusing to the original position. However, the second-order expansion in P_a fails to predict the right refocusing time and finer details in the probability distribution, although the agreement can be improved by fine-tuning the parameters β and w . The full expression of P is, instead, in good agreement with the experiment, as well as with a full QW simulation, except for the emergence of fringe patterns, which would require including the polarization degree of freedom in the description and, in particular, the input polarization state. We also show the evaluation of $P(m, t)$ for a minimal number of terms contributing to the sum in Eq. (S1). As shown in the Methods, the basic features of the breathing dynamics are captured considering only 3 eigenstates for $q_0 = \pi$ and 4 eigenstates for $q_0 = 0$.

S2. CONNECTION BETWEEN THE WAVEFUNCTION ON THE INFINITE AND CYCLIC LATTICE.

Here, we show that the wavefunction calculated for the infinite lattice case can be used to derive the expression of the wavefunction on the cyclic lattice. To retrieve the latter, we prove that it is sufficient to coherently add the contributions of all the lattice sites spaced by N . To model a quantum walk constrained to a ring consisting of N discrete lattice sites, we restrict the allowed momenta to a finite set of discrete Bloch momenta $q_n = 2\pi n/N$, where $n = 0, 1, \dots, N-1$. This momentum-space discretizations is enforced by the projection operator $P_N = \sum_{n=0}^{N-1} |q_n\rangle\langle q_n|$. Applying P_N to the infinite-lattice state yields the finite-lattice state at time t : $|\psi_N(t)\rangle = P_N|\psi_\infty(t)\rangle = \sum_{n=0}^{N-1} \phi_w(q_n)|q_n\rangle \otimes U_{q_n}^t|\phi_c\rangle$, where $\phi_w(q_n)$ is the momentum wavefunction.

In the discrete position basis defined by orthonormal states $\{|x_m\rangle\}_{m=0}^{N-1}$, where the overlap with momentum states is given by $\langle x_m | q_n \rangle = e^{iq_n x_m} / \sqrt{N}$, the matrix elements of the projection operator become: $\langle x_m | P_N | x_{m'} \rangle = \sum_{r \in \mathbb{Z}} \delta_{m', m+rN}$, with r an integer. Consequently, the finite-lattice wavefunction in the discrete position basis is

$$\psi_N(x_m, t) = \sum_{r \in \mathbb{Z}} \psi_\infty(x_m + rN, t). \quad (\text{S3})$$

Note that the summation enforces the periodic boundary condition $\psi_N(x + N) = \psi_N(x)$. According to Eq. (S3), the cyclic wavepacket is obtained by taking the free-space wavefunction $\psi_\infty(x, t)$ on the infinite line and wrapping it around the ring by adding up all of its images shifted by every integer multiple of N . This approach allows one to obtain an analytical expression of the probability distribution of the cycle when the energy dispersion can be expanded to second order in q .

Gaussian State. As an application, we derive the closed-form expression for the evolution of Gaussian wavepackets. We focus on an experimentally relevant case where the walker is initialized in a Gaussian state $\phi_w(q) = \frac{1}{(2\pi\sigma_q^2)^{1/4}} \exp[-\frac{(q-q_0)^2}{4\sigma_q^2}]$. As in the Methods section, we assume a constant polarization and smoothly varying eigenstates. Hence, we can neglect the “coin” terms. Under arbitrary dispersion $E(q)$, the evolved state on the infinite lattice is

$$\psi_\infty(x, t) = \frac{1}{\sqrt{2\pi}} \int_{-\pi}^{\pi} dq \phi_w(q) e^{iqx-itE(q)}. \quad (\text{S4})$$

Inserting the integral form of ψ_∞ in Eq. (S3) yields

$$\psi_N(x, t) = \frac{1}{\sqrt{2\pi}} \sum_{r \in \mathbb{Z}} \int_{-\pi}^{\pi} dq \phi_w(q) e^{iq(x+rN)-itE(q)}.$$

Swapping sum and integral operators, and applying the identity $\sum_{r \in \mathbb{Z}} e^{iqrN} = \frac{2\pi}{N} \sum_{m \in \mathbb{Z}} \delta\left(q - \frac{2\pi m}{N}\right)$, we obtain

$$\psi_N(x, t) = \frac{1}{\sqrt{2\pi}} \int dq \phi_w(q) e^{iqx-itE(q)t} \frac{2\pi}{N} \sum_{m \in \mathbb{Z}} \delta(q - q_m).$$

Performing the δ -integral gives

$$\psi_N(x, t) = \frac{1}{\sqrt{N}} \sum_{m=-\infty}^{\infty} \phi_w(q_m) e^{iq_m x - itE(q_m)}.$$

From this, we can also obtain the on-ring probability density $P_N(x, t) = |\psi_N(x, t)|^2$:

$$P_N(x, t) = \sum_{r \in \mathbb{Z}} C_r(t) e^{i \frac{2\pi r}{N} x},$$

where we have defined the correlation coefficients

$$C_r(t) = \frac{1}{N} \sum_{n \in \mathbb{Z}} \phi_w(q_{n+r}) \phi_w^*(q_n) e^{-it[E(q_{n+r}) - E(q_n)]},$$

with $C_{-r}(t) = C_r^*(t)$ ensuring $P_N(x, t)$ is real. For a Gaussian wavepacket, the correlation function assumes the following form:

$$C_r(t) = e^{-\frac{(r\Delta q)^2}{4\sigma_q^2}} f_r,$$

with $f_r = \frac{1}{N\sqrt{2\pi\sigma_q^2}} \sum_{n \in \mathbb{Z}} \exp\left[-\frac{(q_n-q_0)^2}{2\sigma_q^2} - \frac{r\Delta q(q_n-q_0)}{2\sigma_q^2} - it(E(q_{n+r}) - E(q_n))\right]$. The factor $\propto e^{-(r\Delta q)^2/(4\sigma_q^2)}$ suppresses large- $|r|$ harmonics.

Assume now the energy dispersion is smooth enough to be Taylor-expanded to the second order as $E(q) \approx E(q_0) + v_g(q - q_0) + \frac{D}{2}(q - q_0)^2$, where $v_g := E'(q_0)$ is the group velocity, and $D := E''(q_0)$ is the dispersion coefficient that quantifies curvature in the energy spectrum. Starting from Eq. (S4) and performing a straightforward Gaussian integration, we obtain

$$\psi_\infty(x, t) = \langle x | \psi(t) \rangle = \mathcal{N}(t) e^{i(q_0 x - tE_0)} \exp\left[-\frac{(x - v_g t)^2}{4A(t)}\right], \quad (\text{S5})$$

where $\mathcal{N}(t) = \frac{1}{(2\pi\sigma_q^2)^{1/4}} \sqrt{\frac{\pi}{A(t)}}$ is a normalization factor and $A(t) = \frac{1}{4\sigma_q^2} + i\frac{tD}{2}$. Plugging Eq. (S5) into Eq. (S3), we obtain the closed-form wavefunction for the cyclic walk:

$$\psi_N(x_m, t) = \frac{1}{\sqrt{S(t)}} \psi_\infty(x_m, t) \Theta_3(z(t), \gamma(t)), \quad (\text{S6})$$

where $\Theta_3(z, \gamma) = \sum_{\ell=-\infty}^{\infty} \gamma^{\ell^2} e^{2i\ell z}$ is the Jacobi Theta function, with $z(t) = \frac{q_0 N}{2} + i \frac{(x_m - v_g t) N}{4A(t)}$ and $\gamma(t) = \exp\left[-\frac{N^2}{4A(t)}\right]$, and normalization $\mathcal{S}(t) = \frac{N}{\sqrt{2\pi}\sigma_x(t)}\Theta_3\left(\frac{q_0 N}{2}, |\gamma(t)|\right)$.

As an immediate consequence of Eq. (S6), one can find the probability distribution and fidelity for the cyclic walk as

$$P_N(x_m, t) = \frac{1}{\mathcal{S}(t)} P_\infty(x_m, t) |\Theta(z(t), q(t))|^2,$$

with

$$P_\infty(x, t) = \frac{1}{\sqrt{2\pi\sigma_x^2(t)}} \exp\left[-\frac{(x - v_g t)^2}{2\sigma_x^2(t)}\right].$$

S3. SUPPLEMENTARY FIGURES

Figure S1 shows the 1D breathing dynamics at $v_g = 0$ under different approximations. From left to right insets: scalar approximation, second-order expansion of the energy dispersion, and 3 or 4-wave expansion.

Figure S2 shows a detailed experimental setup.

Figure S3 shows all the results from the QW on the torus, compared with theory.

Figure S4 shows all the results from the QW on the cylinder, compared with theory.

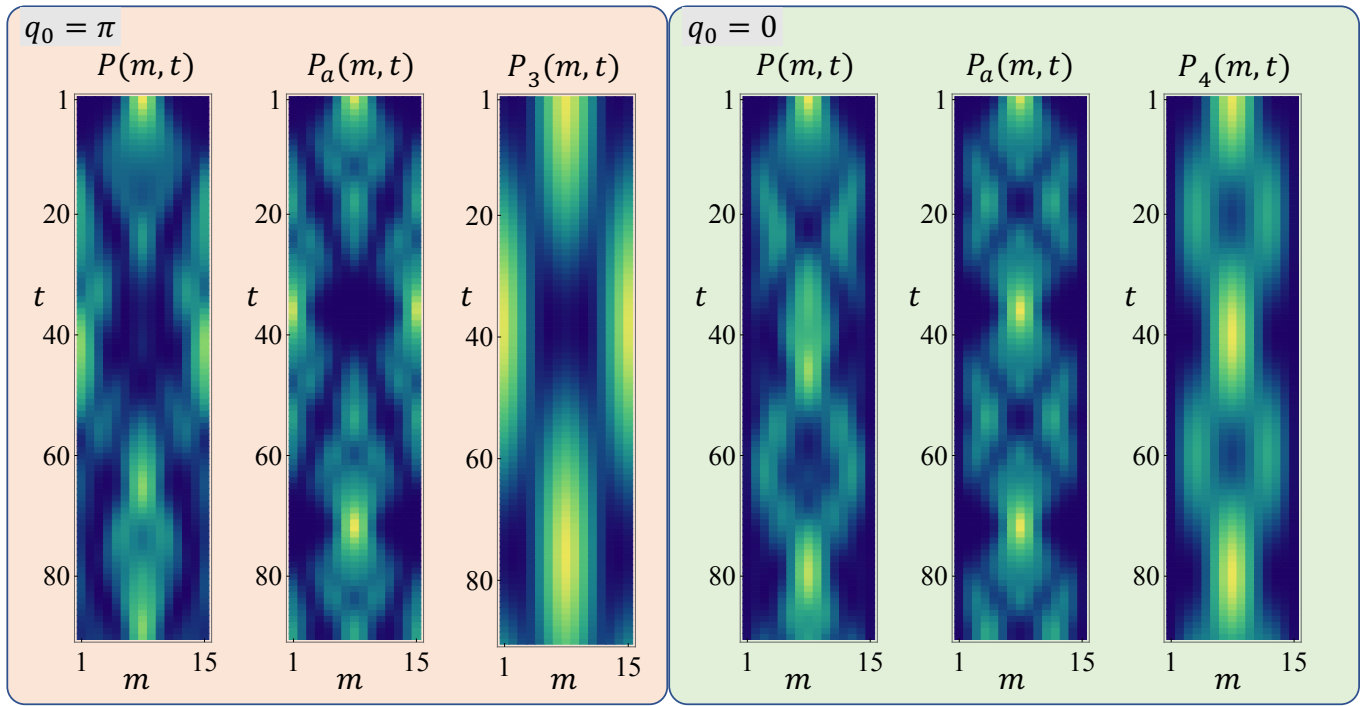


Figure S1. Breathing dynamics of scalar wavepackets with $v_g = 0$. $P(m, t)$ corresponds to Eq. (S1). $P_a(m, t)$ is evaluated from Eq. (S2) expanding the energy dispersion to second order. $P_{3/4}(m, t)$ are obtained by considering only the 3 (4) values of q_h closest to q_0 in Eq. (S1) and illustrate the trend calculated in the Methods (Sec. V E).

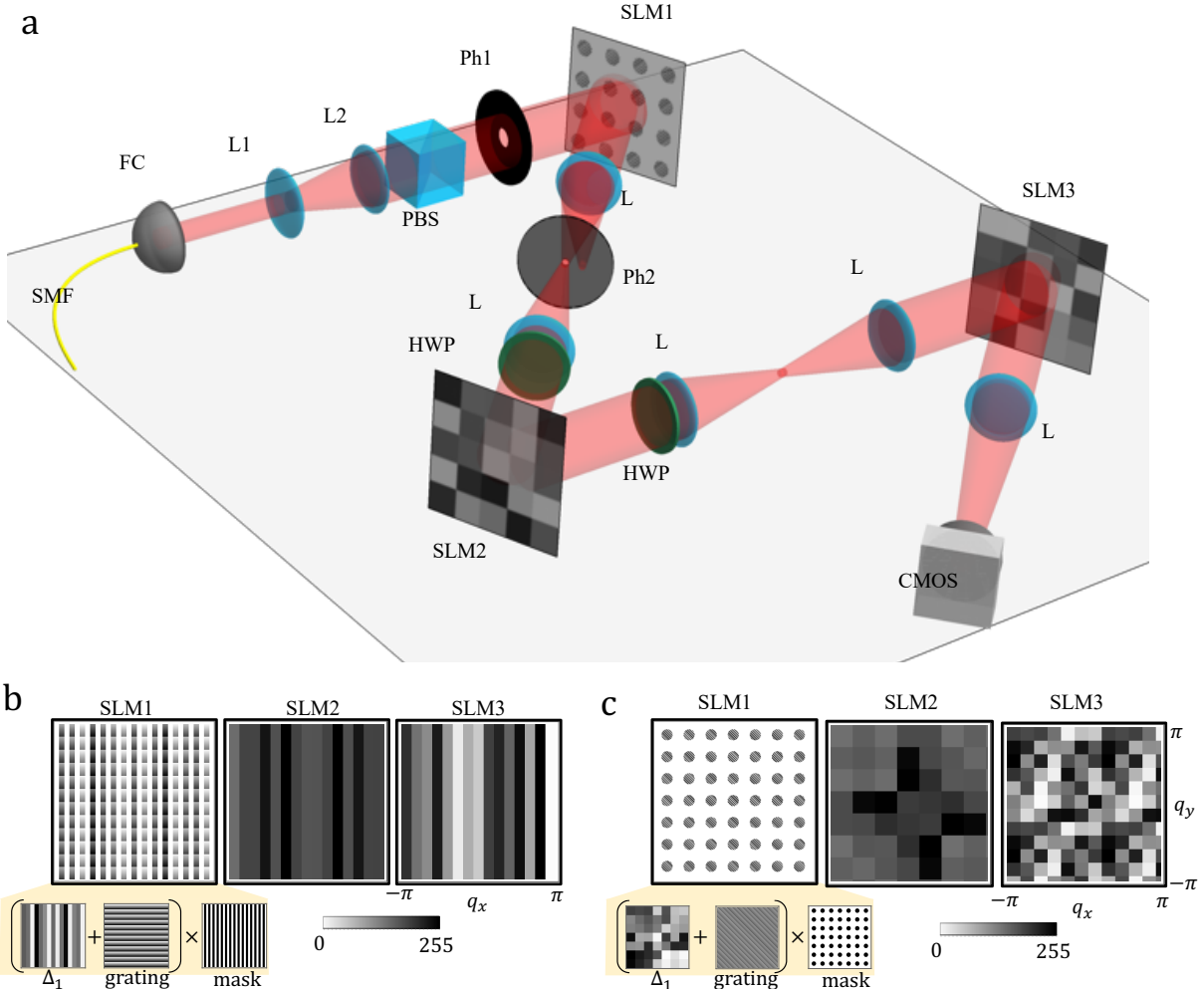


Figure S2. Detailed experimental setup. SMF: single-mode fiber. FC: Fiber output coupler. L1 and L2: beam magnification stage. PBS: Polarizing beam splitter. Ph1: pinhole that allows choosing the width $2/w$ of the input Gaussian states. L: Lens. Ph2: pinhole selecting the first diffraction order from SLM1. HWP: half-wave plates rotated at $\pm 22.5^\circ$ with respect to the extraordinary axis of SLM1. CMOS: camera used to measure far-field intensity distributions. b.-c. Examples of phase masks applied on each SLM. The SLM1, combined with Ph2, simultaneously encodes part of the unitary process and the structuring of the input state into an array of spots using the combination of masks illustrated in the inset.

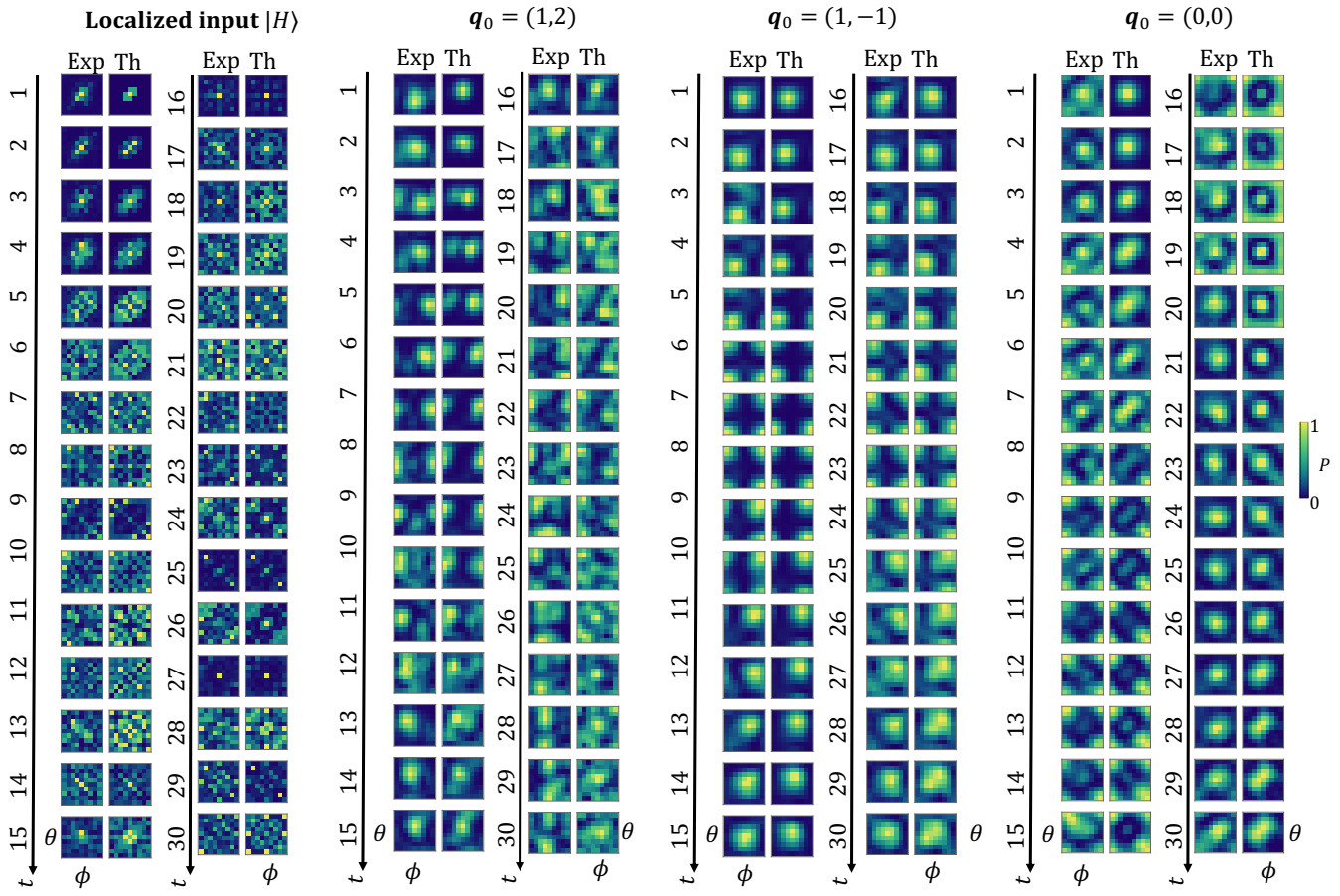


Figure S3. QWs on a torus for initially localized states and wavepackets. Experimental and theoretical QW distributions on a torus with 9x9 lattice sites over 30 time steps. Initial states are all horizontally polarized and prepared either as localized states or as wavepackets. The theory assumes a Gaussian wavepacket.

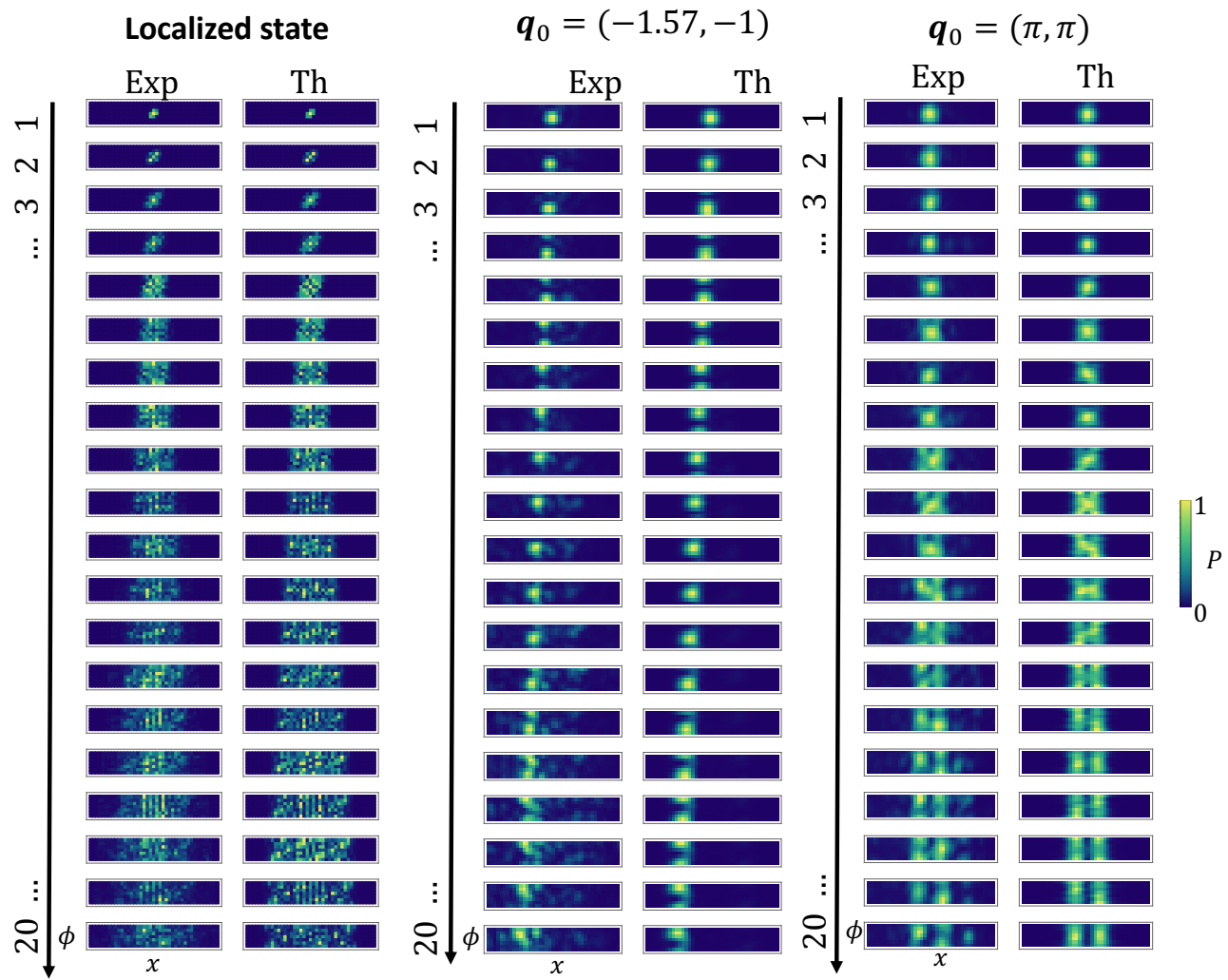


Figure S4. QWs on a cylinder for initially localized states and wavepackets. Experimental and theoretical QW distributions on a cylinder, with 7 lattice sites in the cyclic direction over 30 time steps. Initial states are all horizontally polarized and prepared either as localized states or as wavepackets. The theory assumes a Gaussian wavepacket.